

## Local atomic environment parameters and magnetic properties of disordered crystalline and amorphous iron-silicon alloys

This article has been downloaded from IOPscience. Please scroll down to see the full text article.

1992 J. Phys.: Condens. Matter 4 7597

(<http://iopscience.iop.org/0953-8984/4/37/007>)

View [the table of contents for this issue](#), or go to the [journal homepage](#) for more

Download details:

IP Address: 171.66.16.96

The article was downloaded on 11/05/2010 at 00:33

Please note that [terms and conditions apply](#).

## Local atomic environment parameters and magnetic properties of disordered crystalline and amorphous iron-silicon alloys

E P Elsukov†, G N Konygin†, V A Barinov‡ and E V Voronina‡

† Physical-Technical Institute, Russia Academy of Sciences, Ural Branch, Kirov Street 132, Izhevsk 426001, Russia

‡ Institute of Metal Physics, Russia Academy of Sciences, Ural Branch, Kovalevskaya's Street 18, Ekaterinburg 620219, Russia

Received 7 February 1992

**Abstract.** The dependences of the specific saturation magnetization  $\sigma(C)$ , magnetic ordering temperature  $T_C(C)$ , average hyperfine field  $\bar{H}(C)$  and average isomer shift  $\delta(C)$  on Si concentration are measured in crystalline Fe-Si alloys disordered by mechanical crushing. It is shown that topological disordering does not determine the magnetic properties. The peculiarities found are explained in terms of the local atomic structure parameters depending on the number of Si nearest neighbours of an Fe atom.

### 1. Introduction

In studying the magnetic properties of disordered crystalline (DC) and amorphous transition-metal-sp element (T-sp) alloys the investigation of the influence of the sp-element concentration, the interatomic bond type and the topological and chemical disorder on the properties of these alloys has special significance. However, the role of each factor mentioned above is not clearly understood yet for the following reasons.

- (a) The range of amorphous alloy concentrations is limited.
- (b) There is no comparison of the magnetic parameters of the samples in amorphous and DC states available in the literature.
- (c) There are certain difficulties in interpreting the experimental results.

All this makes it necessary to carry out systematic studies of binary systems which can be produced in both DC and amorphous states in as wide as possible a concentration range. From this point of view the most suitable models are Fe-Si alloys. The results of investigating the magnetic properties of DC Fe-Si alloys with less than 12 at.% Si [1-7] and amorphous Fe-Si films with more than 25 at.% Si [8-11] are known at present. In [12, 13] it was shown that by means of mechanical working in a mill a DC state could be easily obtained for Fe-Si alloys with more than 10 at.% Si. Thereby one can carry out a detailed analysis of the magnetic properties of alloys in a wide concentration range both with topological and chemical disorder and with only chemical disorder. Mössbauer spectroscopy was used to determine the relationship between the magnetic properties and the local atomic environment

characteristics by analogy to the well known Jaccarino-Walker [14] model. A number of theoretical [15] and experimental studies of disordered alloys of transition metals such as Fe-V [16, 17], as well as ordered Fe-Al [18] and Fe-Si [19] alloys in which integral magnetic parameters of the alloys were interpreted in terms of the local atomic environment characteristics, prove that this approach is also successful for studying T-sp disordered systems.

In this work the results of studying the macroscopic and local atomic structure, and the average and local magnetic and hyperfine parameters in DC Fe-Si alloys with up to 70 at.% Si are presented. The results are compared with the data obtained for amorphous Fe-Si films.

## 2. Experiment

Fe-Si alloys with 1.8, 4.0, 6.0, 8.6, 9.9, 11.2, 13.0, 15.0, 17.6, 21.2, 24.2, 26.6, 28.0, 30.6, 33.0, 37.5, 50.0 and 70.0 at.% Si were melted in a vacuum induction furnace from pure components (99.99% Fe and 99.99% Si). The ingots of the alloys were homogenized for 6 h at 1423 K. The alloys produced were tested by chemical and x-ray analysis. The error in determining the Si concentration did not exceed 0.3 at.%.

To obtain a DC state by means of mechanical working, samples with a previously fixed single-phase state were used. The alloys with up to 25 at.% Si were annealed at 1073 K (for 1 h) to obtain maximal ordering of the  $D0_3$  type; this was followed by slow cooling to 773 K and then the alloys were kept at this temperature for 4 h. The alloys with more than 25 at.% Si and up to 33 at.% Si were quenched from 1350 K into salt water. Under these conditions a single-phase state with a metastable superlattice of the  $D0_3$  type was obtained in the samples as was reported in [19, 20]. The sample with 37.5 at.% Si was annealed at 1173 K (for 48 h), quenched into salt water, ground into particles of 50–100  $\mu\text{m}$ , annealed once again under the same conditions and finally quenched again. This procedure provided the maximally possible homogeneous state in this alloy with a hexagonal phase  $\text{Fe}_5\text{Si}_3$ . According to the equilibrium diagram of the states [21], the FeSi and  $\alpha\text{-Fe}_{0.86}\text{Si}_2$  phases were found in alloys with 50 and 70 at.% Si, respectively. Being highly ductile, the powder samples with up to 10 at.% Si were prepared by sawing massive ingots. Mechanical working of the alloys with more than 10 at.% Si was carried out for 3 or 4 h in a planetary Pulverizette ball mill with mortars and balls made of WC. The average size of the powder particles was estimated according to the secondary-electron image obtained with a Jamp-10S Auger spectrometer in scanning electron microscope mode and was found to be equal to 1–2  $\mu\text{m}$ .

X-ray analysis was carried out at room temperature using Fe  $K_\alpha$  radiation with an Mn filter. The Mössbauer spectra were recorded at 77 K with a constant-acceleration spectrometer (NGRS-4M), the  $\gamma$  source being  $^{57}\text{Co}$  in a Cr matrix. The spectra were processed in two steps. First, the hyperfine magnetic field distribution  $P(H)$  was obtained and the average hyperfine field values  $\bar{H}$  were defined using the usual algorithm for solving inverse incorrect problems [22]. The best fit of the Mössbauer spectra of the samples with an Si content  $C$  of up to 28 at.% was obtained using a linear dependence between the isomer shift  $\delta$  and hyperfine field  $H$ ; for higher concentrations the average isomer shift  $\bar{\delta}$  was used. Second, taking into account the peculiarities of the  $P(H)$ - and  $\delta(H)$ -dependences, the spectra analysis was performed by a discrete least-squares method. This procedure provided

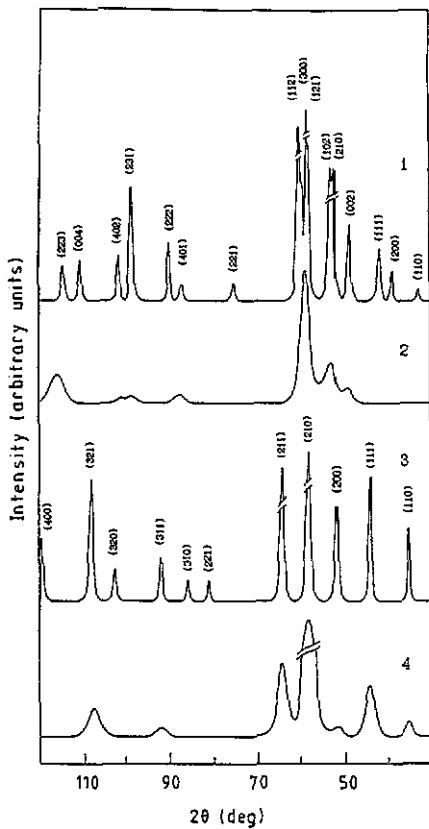


**Figure 1.** X-ray diffraction patterns of Fe-Si alloys with 37.5 and 50.0 at.% Si at 300 K before (curves 1 and 3) and after (curves 2 and 4) mechanical working.

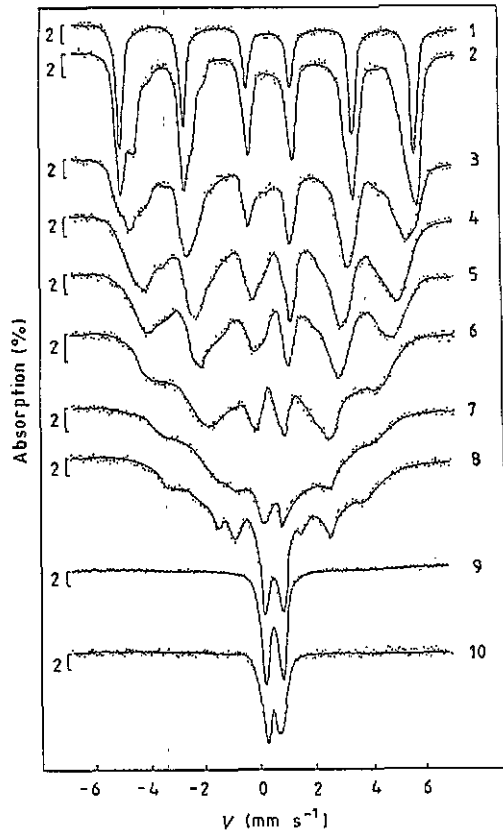


**Figure 2.** Mössbauer spectra of Fe-Si alloys at 77 K after mechanical working: curve 1, 0 at.% Si; curve 2, 6.0 at.% Si; curve 3, 13.0 at.% Si; curve 4, 21.2 at.% Si; curve 5, 24.5 at.% Si; curve 6, 28.0 at.% Si; curve 7, 33.0 at.% Si; curve 8, 37.5 at.% Si; curve 9, 50.0 at.% Si; curve 10, 70.0 at.% Si.

a more reliable determination of the local hyperfine magnetic fields  $H_K$  and local configuration probabilities  $P_K$ .

The values of the specific saturation magnetization  $\sigma$  of the alloys were obtained by linear extrapolation of the  $\sigma(H)$ -dependences to  $H = 0$ , which were measured with a vibration magnetometer at 4.2 K. The temperature of magnetic ordering was estimated from Mössbauer spectroscopy and magnetic measurements.

### 3. Results and discussion

The structure of crushed Fe-Si alloys was checked by x-ray diffraction and Mössbauer spectroscopy.

Only broadened peaks of a BCC (A2) lattice structure were recorded in the diffraction diagrams of the samples with an Si content of up to 30.6 at.%; ordered B2 or D0<sub>3</sub> superlattice lines were not found. The diffraction diagrams of the samples with 33.0, 37.5, 50.0 and 70.0 at.% Si had fewer lines than those of the initial state for these alloys, as seen in figure 1 for the samples with 37.5 and 50.0 at.% Si.

The Mössbauer spectra of crushed alloys (figure 2) essentially differ from the known spectra for ordered samples with an Si concentration of up to 33 at.% [13, 23–25] and for the phases  $\text{Fe}_5\text{Si}_3$  [26],  $\text{FeSi}$  [27],  $\alpha\text{-Fe}_{0.86}\text{Si}_2$  [28] and  $\beta\text{-Fe}_2\text{Si}$  [29]. On the other hand, the spectra for alloys with more than 20 at.% Si illustrated in figure 2 were similar to those for the amorphous Fe–Si films [9–11]. A great number of non-equivalent positions characteristic of an atomic disordered state is clearly seen in the hyperfine magnetic field distribution  $P(H)$  obtained from the spectra (figure 3). To study the characteristics of the local atomic environment in detail the Mössbauer spectra were processed by a discrete method with a number of sextets equal to the number of centres in the local hyperfine field distribution found in the  $P(H)$ -functions. Only those maxima (figure 3) where amplitude changed regularly with increasing Si content in the alloys were considered. The data obtained concerning the probabilities  $P_K^Z$  of the local environment of Fe atoms ( $K$  is the number of Si nearest neighbours of the Fe atom) are illustrated in figure 4. In the same figure the full curves show the probabilities  $P_K^Z$  for the coordination numbers  $Z = 8$  (curves 1) and  $Z = 14$  (curves 2) calculated under the assumption of random distribution of atoms of alloy components according to the equation

$$P_K^Z(C) = \binom{Z}{K} C^K (1-C)^{Z-K} \quad (1)$$

From the figure it is seen that the experimental values agree with curves 1 ( $Z = 8$ ) at  $C \leq 15$  at.% Si and with curves 2 ( $Z = 14$ ) when  $C \geq 33$  at.% Si.

Let us assume that in the concentration range from 15 to 33 at.% a disordered state with a random set for coordination numbers  $Z$  from 8 to 14 and with a random distribution of Fe and Si atoms for every  $Z$  is realized. In this case the values of probabilities of the local configuration can be calculated according to the relations

$$P_K^{Z=8-14}(C) = \sum_{n=0}^6 \binom{6}{n} C_{np}^n (1-C_{np})^{6-n} \binom{8+n}{K} C^K (1-C)^{8+n-K} \quad (2)$$

$$C_{np} = (C - 0.15)/0.18. \quad (3)$$

The calculated values  $P_K^{Z=8-14}$  (curves 3 in figure 4) account for the experimental results of  $P_K$  in the concentration range from 15 to 33 at.% Si.

Hence, x-ray and Mössbauer studies allow us to draw the conclusion that Fe–Si alloys are in a DC state after mechanical working. However, with increasing Si concentration a transition from a disordered BCC lattice with  $Z = 8$  to a disordered crystalline structure with  $Z = 14$  occurs.

The specific saturation magnetization data  $\sigma$  and magnetic ordering temperature values  $T_C$  obtained for DC Fe–Si alloys are illustrated in figures 5 and 6, respectively. The same figures show the well known reported data for DC alloys with less than 12 at.% Si [1–7] and for amorphous films with  $C > 25$  at.% Si [9, 10]. Note that in the present work we have failed to measure  $T_C$  for DC alloys with an Si content from 12 to 23 at.%. For these alloys the temperature of magnetic ordering exceeds the temperature of the disorder–order transition (according to [30], about 600 K) and thus, while measuring  $T_C$ , the alloys were ordered according to the  $\text{D0}_3$  type. The values of  $\sigma(C)$  and  $T_C(C)$  for the DC alloys rich in Si agree with the data for amorphous films and are much lower than could be expected judging by curves 1 in figures 5 and 6, which are linear extrapolations of the initial part.

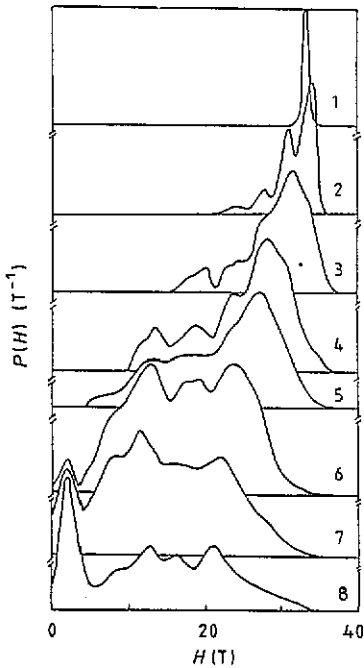


**Figure 3.** Hyperfine field distribution functions  $P(H)$  of Fe-Si alloys after mechanical working: curve 1, 0 at.% Si; curve 2, 6.0 at.% Si; curve 3, 13.0 at.% Si; curve 4, 21.2 at.% Si; curve 5, 24.5 at.% Si; curve 6, 28.0 at.% Si; curve 7, 33.0 at.% Si; curve 8, 37.5 at.% Si.

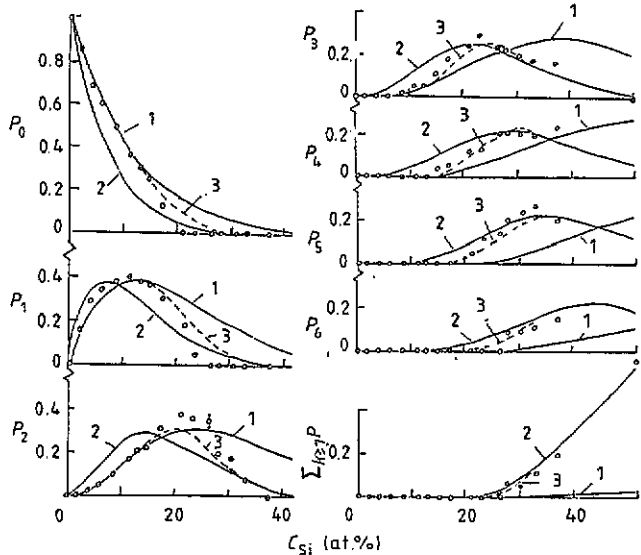


**Figure 4.** Concentration dependences of the local configuration probabilities  $P_K(C)$  in Fe-Si alloys after mechanical working:  $\circ$ , experimental data; curves 1, values calculated for a binomial distribution of atoms with  $Z = 8$ ; curves 2, values calculated for a binomial distribution of atoms with  $Z = 14$ ; curves 3, values calculated for a random set of the coordination numbers  $Z$  from 8 to 14 with binomial distributions of atoms over each  $Z$ .

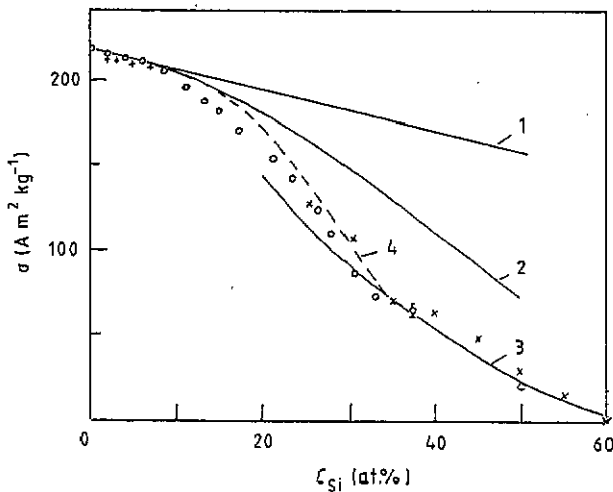


**Figure 5.** Specific saturation magnetization of disordered crystalline and amorphous Fe-Si alloys at 4.2 K:  $\circ$ , this work; +, [3, 4];  $\times$ , [9, 10]; curve 1, linear extrapolation; curve 2, values calculated for  $Z = 8$ ; curve 3, values calculated for  $Z = 14$ ; curve 4, values calculated for  $Z = 8-14$ .

The hyperfine magnetic field distribution functions  $P(H)$  (figure 3) obtained from the Mössbauer spectra allow us to find the mean values  $\bar{H}$  of the hyperfine magnetic

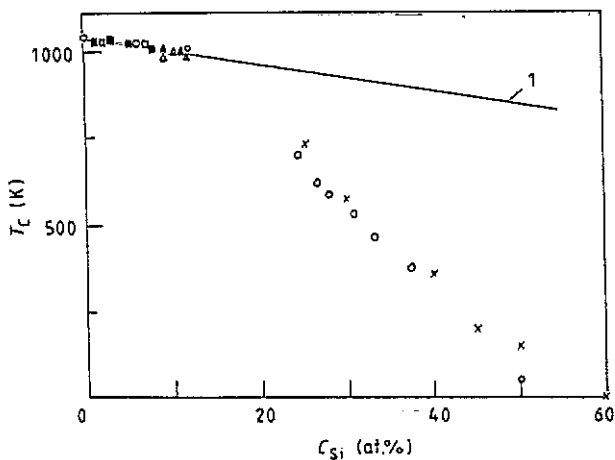


Figure 6. Curie temperature of disordered crystalline and amorphous Fe-Si alloys: O, this work; □, [1]; ▲, [2]; ■, [4]; △, [5-7]; x, [9, 10].

fields using the equation

$$\overline{H}(C) = \int H P(H) dH \quad (4)$$

without any prior information concerning the characteristics of the local atomic environment. Here,  $\overline{H}$  is analogous to the integral magnetic parameters  $\sigma$  and  $T_C$ . In figure 7 the values of  $\overline{H}$  found for 77 K are indicated as open circles. On comparing the  $\overline{H}$  data for DC and amorphous [9-11] alloys, one can draw the conclusion that  $\overline{H} = 0$  for 50.0 at.% Si, which disagrees with the results of the magnetic measurements presented in figures 5 and 6;  $\sigma(C)$  and  $T_C(C) \rightarrow 0$  for 60 at.% Si. To specify the type of dependence  $\overline{H}(C)$  in the alloys with a high Si content the spectra of the alloy with 50 at.% Si in its initial state and after mechanical working in mill were obtained at 6 K. Mechanical working was found to give rise to a magnetic component of weak intensity with a maximum field not exceeding 15 T. The value  $\overline{H} = 5$  T calculated according to equation (4) for a milled alloy with 50 at.% Si is indicated by a full circle in figure 7. The considerable difference from  $\overline{H} = 0$  for an amorphous film with 50 at.% Si is due to high-temperature (about 100 K) measurements of Mössbauer spectra in [9, 10]. Thus, the critical value of the Si content at which  $\overline{H} = 0$  could be estimated for DC and amorphous alloys is 60 at.%. On the whole the dependence  $\overline{H}(C)$  is non-linear. At  $C \simeq 10$  at.% Si there is a deviation from curve 1 in figure 7 obtained by linear extrapolation of the initial part. The change in the slope angle of  $\overline{H}(C)$  takes place in the concentration regions at about 15 and 33 at.% Si.

The values of the average isomer shifts  $\overline{\delta}$  relative to  $\alpha$ -Fe found in the course of obtaining the  $P(H)$ -functions are presented in figure 8 together with the data from the literature on amorphous films [9-11] and DC alloys of low Si concentration [23]. Within the limits of measurement errors no difference was found between  $\overline{\delta}$  for the amorphous and DC alloys.

Thus, from the coincidence of the concentration dependences  $\sigma(C)$ ,  $T_C(C)$ ,  $\overline{H}(C)$  and  $\overline{\delta}$  for amorphous and DC samples we can draw one of the main conclusions of this work: topological disorder does not affect the fundamental magnetic properties of Fe-Si alloys.

To explain the concentration dependences of the magnetic properties, let us compare the experimental values of the average parameters  $\sigma(C)$  and  $\overline{H}(C)$  with

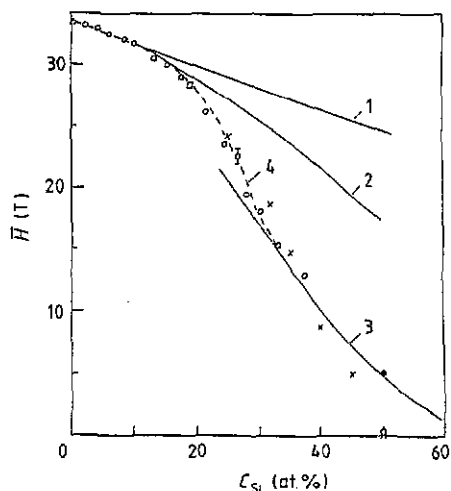


**Figure 7.** The average hyperfine magnetic fields in disordered crystalline and amorphous Fe-Si alloys: O, this work (77 K); ●, this work (6 K); x, [9, 10]; □, [11]; curve 1, linear extrapolation; curve 2, values calculated for  $Z = 8$ ; curve 3, values calculated for  $Z = 8-14$ .

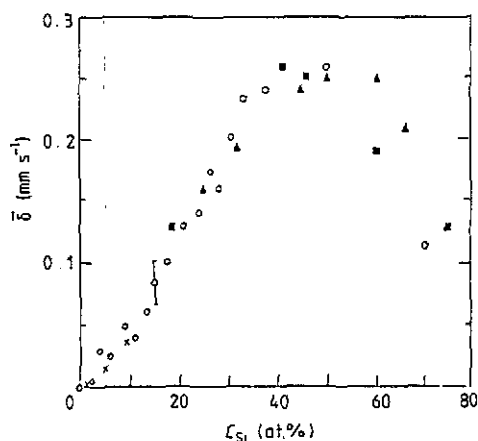


**Figure 8.** The average isomer shift values relative to  $\alpha$ -Fe in disordered crystalline and amorphous Fe-Si alloys: O, this work; x, [23]; ■, [11]; ▲, [9, 10].

the values calculated by means of the following characteristics of the local atomic environment of Fe atoms:  $m_K$ , local magnetic moments of an Fe atom;  $H_K$ , local hyperfine fields on an  $^{57}\text{Fe}$  atom nucleus;  $P_K^Z$ , probabilities of local configurations of a Fe atom with  $K$  atoms of Si as nearest neighbours:

$$\bar{H}(C) = \sum_K H_K P_K^Z(C) \quad (5)$$

$$\sigma(C) = A(C) \sum_K m_K P_K^Z(C) \quad (6)$$

where  $A$  is the coefficient of proportionality between  $\sigma$  and  $m$ .

Not only  $P_K^Z$  but also  $H_K$  were found by a discrete computational method of processing Mössbauer spectra. The analysis of the local hyperfine field  $H_K$  data proves that they actually do not depend on the concentration of Si in the alloys. When averaged over the concentration range, the  $H_K$ -values considered (figure 9, curve 1) demonstrate a non-linear dependence on the number  $K$  of Si atoms in the first coordination shell. With  $K \geq 3$ , one observes a sharper drop in  $H_K$ , with  $H_K = 0$  for  $K = 7$ . The non-linear behaviour of the local hyperfine magnetic fields is brought about by the change in interatomic Fe-Si bonds from (Fe) 4sp-(Si) 3p for the first two Si nearest-neighbour atoms of an Fe atom to (Fe) 3d-(Si) 3p for the third and subsequent atoms [31, 32].

The form of  $m_K(K)$  was derived from the following experimental data.

(1) The results of magnetic neutronographic measurements [33, 34] for a stoichiometric ordered  $\text{Fe}_3\text{Si}$  alloy show the presence of two local magnetic moments on Fe atoms in accordance with their two non-equivalent sites in a  $\text{D0}_3$  unit cell  $m_0 = (2.2-2.4)\mu_B$  and  $m_4 = (1.2-1.4)\mu_B$ .



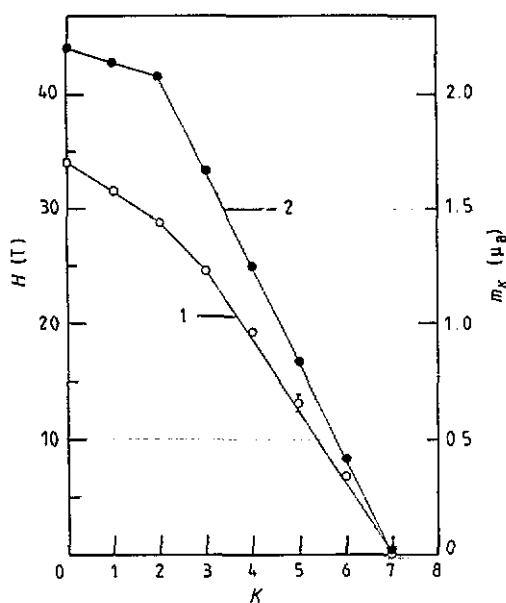


Figure 9. The dependences of the local hyperfine field  $H_K$  (curve 1) and magnetic moments  $m_K$  per Fe atom (curve 2) on the number of Si nearest neighbours of an Fe atom for disordered crystalline Fe-Si alloys.

(2) According to [30, 35] there is little difference between  $m_1$ ,  $m_2$  and  $m_0$ ; they slightly decrease relative to  $m_0 = 2.2\mu_B$  as shown in [35], by approximately  $0.06\mu_B$  for each of the first two Si atoms in the nearest Fe-atom environment.

(3) In contrast with [35], where it was assumed that the local magnetic moment on an Fe atom became zero with eight Si atoms, in this work according to the Mössbauer studies carried out it was assumed that  $m_7 = 0$ . The latter does not contradict the known data [36] in accordance with which a monosilicide FeSi with a single local configuration—seven Si atoms as nearest neighbours of an Fe atom—is a paramagnet up to liquid-helium temperature.

The  $m_K(K)$ -dependence plotted in figure 9 (curve 2) agrees with that of [35] except for  $m_7 = 0$  and considerably differs from the 'step' Jaccarino-Walker [14] model.

The dependences  $\bar{H}(C)$  and  $\sigma(C)$  for  $Z = 8$  calculated according to equations (5) and (6) are presented as curves 2 in figures 7 and 5, respectively. It is obvious that the non-linear behaviour of  $H(K)$  and  $m(K)$  allows us to explain the non-linearity of  $\bar{H}(C)$  and  $\sigma(C)$  in the region of 10 at.% Si. At the same time, for an Si content greater than 15 at.%, the amount by which the calculated dependences  $\bar{H}(C)$  and  $\sigma(C)$  exceed the experimental values increases as the Si content increases. On the other hand,  $\bar{H}(C)$  and  $\sigma(C)$  calculated for  $Z = 14$  and shown by curves 3 in figures 5 and 7 agree well with the experimental values of  $\bar{H}$  and  $\sigma$  obtained for DC alloys in this work and with those in [9, 10] for amorphous Fe-Si films for  $C \geq 33$  at.% Si. Thereby, the facts that the hyperfine magnetic field as well as the specific saturation magnetization approach zero in DC and amorphous Fe-Si alloys in the region of 60 at.% Si is accounted for by the character of the dependences of  $H(K)$  and  $m(K)$  in which  $H_K = 0$  and  $m_K = 0$  for  $K = 7$ , as well as by the realization of a local atomic structure with the coordination number for the nearest neighbours of an Fe atom of  $Z = 14$  in the region of high Si concentrations. Finally, in the range of 15–33 at.% Si the experimental results are explained by the  $\bar{H}(C)$ -

and  $\sigma(C)$ -dependences calculated according to equations (2) and (3), using  $P_K^Z(C)$  for a random set of coordination numbers  $Z$  from 8 to 14—curves 4 in figures 5 and 7. Thus, a satisfactory description of the concentration dependences of the magnetic properties of DC Fe-Si alloys is achieved by using a model in which for  $C \leq 15$  at.% Si a disordered BCC lattice with  $Z = 8$  is realized; for  $C = 15$ –33 at.% Si, within the BCC structure, local atomic arrangements with a random set of coordination numbers of the nearest Fe-atom environment from 8 to 14 are formed; with  $C \geq 33$  at.% Si, structures with the coordination number  $Z = 14$  are developed.

The cause of the concentration phase transition which considerably affects the properties of the Fe-Si alloys can be qualitatively understood from the following experimental evidence and considerations. In [25, 37] it was stated that it was prohibited for Si atoms pairs to be at the distance of nearest neighbours in the BCC lattice of equilibrium Fe-Si alloys. As was shown in [38, 39] the occurrence of Si-Si pairs gave rise to the formation of their own 3p bands and, as a result, the interatomic interaction of 3p states acquires considerable importance. One can suppose that at the characteristic interatomic distances of the nearest neighbours (about 0.24 nm) between Si atoms, repulsive forces appear, resulting in local distortion in the BCC lattice. With increasing Si content in alloys and consequently with increasing number of Si-Si pairs, these local distortions eliminate the difference between the first ( $Z = 8$ ) and the second ( $Z = 6$ ) coordination shells in a distorted BCC lattice.

#### 4. Conclusions

(1) The measured concentration dependences of the magnetic properties (specific saturation magnetization  $\sigma$ , Curie temperature  $T_C$  and average hyperfine field  $\overline{H}$ ) and of the isomer shift  $\overline{\delta}$  of DC Fe-Si alloys coincide with those for Fe-Si amorphous films. This proves that topological disorder does not determine the physical properties.

(2) The peculiarities of the concentration dependences found in the regions of 10, 15 and 30 at.% Si can be explained in terms of the local atomic environment parameters. (a) The change in interatomic Fe-Si bonds with three or more Si atoms appearing as nearest neighbours of the Fe atom results in a bend in the dependences of the local characteristics  $H_K$  and  $m_K$  on the number of nearest Si atoms and in their becoming equal to zero with  $K = 7$ . The bend is manifested by non-linear behaviour of the concentration dependences of the macrophysical properties in the region of 10 at.% Si. (b) The change in the local atomic structure character with increasing Si content from 15 to 33 at.%, which is manifested in a change in the coordination number  $Z$  from 8 to 14, results in a sharp drop in the  $\sigma$ - and  $\overline{H}$ -values (with given local parameters  $m_K$  and  $H_K$  when the Si content increases) and their becoming zero at about 60 at.% Si.

(3) The state of alloys in the concentration range from 15 to 33 at.% Si can be characterized by a random set of coordination numbers  $Z$  from 8 to 14 with a statistical distribution of Fe and Si atoms for each  $Z$ .

#### Acknowledgments

The authors would like to express their gratitude to Dr R A Manapov and Dr F G Vagizov for the assistance rendered in carrying out the low-temperature Mössbauer measurements.

## References

- [1] Fallot M 1936 *Ann. Phys.* **6** 305
- [2] Glaser F W and Iwanick W 1956 *Trans. AIME* **206** 1290
- [3] Parsons D, Sucksmith W and Thompson J E 1958 *Phil. Mag.* **3** 1174
- [4] Arays S 1965 *Phys. Status Solidi* **11** 121; 1968 *Phys. Status Solidi* **33** 683
- [5] Pepperhoff W and Ettwig H-H 1967 *Z. Angew. Phys.* **22** 496
- [6] Pepperhoff W and Ettwig H-H 1968 *Arch. Eisenhüttenwes.* **39** 307
- [7] Ettwig H-H and Pepperhoff W 1972 *Z. Metallk.* **63** 453
- [8] Snimada Y and Kojima H 1976 *J. Appl. Phys.* **47** 4156
- [9] Marchal G, Mangin Ph, Picuch M and Janot Chr 1976 *J. Physique Coll.* **37** C6 763
- [10] Mangin Ph and Marchal G 1978 *J. Appl. Phys.* **49** 1709
- [11] Bansal C, Campbell S J and Stewart A M 1982 *J. Magn. Magn. Mater.* **27** 195
- [12] Elsukov E P, Barinov V A, Galakhov V R, Yurchikov E E and Ermakov A E 1983 *Fiz. Metall. Metalloved.* **55** 337
- [13] Elsukov E P, Barinov V A and Konygin G N 1986 *Fiz. Metall. Metalloved.* **62** 719
- [14] Jaccarino V and Walker L R 1965 *Phys. Rev. Lett.* **15** 258
- [15] Zaborov A V and Medvedev M V 1983 *Phys. Status Solidi b* **116** 227, 511
- [16] Ryzhenko B V and Geld P V 1987 *Fiz. Tverd. Tela* **29** 196
- [17] Shiga M and Nakamura Y J 1982 *J. Phys. F: Met. Phys.* **12** 537
- [18] Ryzhenko B V, Goloborodski B Yu, Zaborov A V and Geld P V 1984 *Fiz. Metall. Metalloved.* **58** 1153
- [19] Elsukov E P, Barinov V A and Konygin G N 1989 *Metallofizika* **11** 52
- [20] Kudiclika H 1977 *Z. Kristallogr.* **145** 177
- [21] Kubashewski O 1982 *Iron Binary Phase Diagrams* (Berlin: Springer)
- [22] Voronina E V, Ershov N V, Ageev A L and Babanov Yu A 1990 *Phys. Status Solidi b* **160** 625
- [23] Stearns M B 1963 *Phys. Rev.* **129** 1136
- [24] Häggström L, Grånäs L, Wäppling R and Devanarayanan S 1973 *Phys. Scr.* **7** 125
- [25] Elsukov E P, Konygin G N and Voronina E V 1990 *Metallofizika* **12** 75
- [26] Shinjo T and Nakamura Y 1963 *J. Phys. Soc. Japan* **18** 797
- [27] Wertheim G 1966 *Effekt Messbauera* (Moscow: Mir)
- [28] Sidorenko F A, Geld P V, El'ner L Yu and Ryzhenko B V 1982 *J. Phys. Chem. Solids* **43** 297
- [29] Dubovtzev I A and Sidorenko F A 1971 *Pis. Zh. Eksp. Teor. Fiz.* **14** 205
- [30] Elsukov E P, Barinov V A, Lapina T P, Galakhov V R and Konygin G N 1985 *Fiz. Metall. Metalloved.* **60** 925
- [31] Elsukov E P and Konygin G N 1989 *Fiz. Metall. Metalloved.* **67** 301
- [32] Elsukov E P, Vorobev Yu N, Trubachev A V and Barinov V A 1990 *Phys. Status Solidi a* **117** 291
- [33] Meinhardt D and Krisement O 1963 *Z. Phys.* **174** 472
- [34] Paoletti A and Passari L 1964 *Nuovo Cimento* **32** 25
- [35] Niculescu V, Litrenta T, Ray K et al 1977 *J. Phys. Soc. Japan* **42** 1538
- [36] Geld P V and Sidorenko F A 1971 *Silitizidym Perekhodnykh Metallov Chervertogo Perioda* (Moscow: Metallurgija)
- [37] Cranshaw T E 1977 *Physica B & C* **86-87** 391
- [38] Anisimov B I, Postnikov A B and Kurmaev E Z 1986 *Fiz. Metall. Metalloved.* **62** 730
- [39] Elsukov E P, Churakov V P, Konygin G N and Bayankin V Y 1991 *Izv. Akad. Nauk USSR, Ser. Metall.* **1** 172